

# Exchange parameters of copper-based quasi-two-dimensional Heisenberg magnets measured using high magnetic fields and muon-spin rotation

P.A. Goddard,<sup>1</sup> John Singleton,<sup>2</sup> P. Sengupta,<sup>3</sup> R.D. McDonald,<sup>2</sup> T. Lancaster,<sup>1</sup> S.J. Blundell,<sup>1</sup> F.L. Pratt,<sup>4</sup> S. Cox,<sup>2</sup> N. Harrison,<sup>2</sup> J.L. Manson,<sup>5</sup> H.I. Southerland,<sup>5</sup> and J.A. Schlueter<sup>6</sup>

<sup>1</sup>*University of Oxford Department of Physics, The Clarendon Laboratory, Parks Road, Oxford OX1 3PU, United Kingdom*

<sup>2</sup>*National High Magnetic Field Laboratory, Los Alamos National Laboratory, MS-E536, Los Alamos, NM 87545, USA*

<sup>3</sup>*Theoretical Division, Los Alamos National Laboratory, Los Alamos, NM 87545, USA*

<sup>4</sup>*ISIS Facility, Rutherford Appleton Laboratory, Chilton, Oxfordshire, OX11 0QX, United Kingdom*

<sup>5</sup>*Department of Chemistry and Biochemistry, Eastern Washington University, Cheney, WA 99004, USA*

<sup>6</sup>*Materials Science Division, Argonne National Laboratory, Argonne, IL 60439, USA*

Pulsed-field magnetization experiments (fields  $B$  of up to 85 T and temperatures  $T$  down to 0.4 K) are reported on nine organic Cu-based two-dimensional (2D) Heisenberg magnets. All compounds show a low- $T$  magnetization that is concave as a function of  $B$ , with a sharp “elbow” transition to a constant value at a field  $B_c$ . Monte-Carlo simulations including a finite interlayer exchange energy  $J_{\perp}$  quantitatively reproduce the data; the concavity indicates the effective dimensionality and  $B_c$  is an accurate measure of the in-plane exchange energy  $J$ . Using these values and Néel temperatures measured by muon-spin rotation, it is also possible to obtain a quantitative estimate of  $|J_{\perp}/J|$ . In the light of these results, it is suggested that in magnets of the form  $[\text{Cu}(\text{HF}_2)(\text{pyz})_2]\text{X}$ , where X is an anion, the sizes of  $J$  and  $J_{\perp}$  are controlled by the tilting of the pyrazine (pyz) molecule with respect to the 2D planes.

PACS numbers: 76.30-v, 75.10.Pq

## I. INTRODUCTION

Systems that can be described by the  $S = \frac{1}{2}$  two-dimensional (2D) square-lattice quantum Heisenberg antiferromagnet model<sup>1,2,3</sup> continue to attract considerable experimental<sup>4,5</sup> and theoretical<sup>6,7,8,9</sup> attention. Recent impetus has been added to this field by suggestions that antiferromagnetic fluctuations from  $S = \frac{1}{2}$  ions on a square lattice play a pivotal role in the mechanisms for superconductivity in the “high  $T_c$ ” cuprates<sup>3,10,11,12,13,14</sup> and other correlated-electron systems<sup>15</sup>; moreover, 2D Heisenberg magnets have been suggested as possible testbeds for processes applicable to quantum computation<sup>4,9</sup>.

Though long-range magnetic order cannot occur above  $T = 0$  in a true 2D Heisenberg system<sup>2,16</sup>, real materials that contain layers approximating to 2D Heisenberg systems<sup>2,4,17,18</sup> invariably possess interlayer coupling that can lead to a finite Néel temperature<sup>4,17,19</sup>. In this context, synthesis of organic complexes containing ions such as  $\text{Cu}^{2+}$ , neutral bridging ligands<sup>4</sup> and coordinating anion molecules<sup>17,18</sup> has proved fruitful in the production of a variety of one- and 2D magnetic systems<sup>17,20,21,22</sup>. The current paper describes high-field magnetization measurements on nine Cu-based quasi-2D Heisenberg magnets that employ pyrazine (pyz) as a neutral bridging ligand<sup>17,18,23</sup>. The data show that the field ( $B$ )-dependent, low-temperature ( $T$ ) magnetization  $M(B)$  shows a characteristic sharp “elbow” feature at the transition to saturation, with a concave curvature at lower  $B$ . Monte-Carlo evaluations of a 2D Heisenberg square lattice with an additional interlayer exchange coupling energy  $J_{\perp}$  reproduce the data quantitatively; the degree of concavity depends on the effective dimensionality of the system,

whilst the field at which the “elbow” occurs is an accurate measure of the in-plane exchange energy  $J$ . Using these  $J$  values in conjunction with Néel temperatures deduced from muon-spin rotation ( $\mu\text{SR}$ ), it is then possible to gain a good estimate of the exchange anisotropy  $|J_{\perp}/J|$  for all of the magnets.

Having established these findings using the whole range of compounds, we suggest that in magnets of the form  $[\text{Cu}(\text{HF}_2)(\text{pyz})_2]\text{X}$ ,<sup>18,19</sup> where X is an anion,  $J$  and  $J_{\perp}$  may be influenced by the tilting of the pyrazine (pyz) molecule with respect to the 2D planes.

## II. EXPERIMENTAL DETAILS

The quasi-2D magnets studied in this work are listed in Table I. The samples are produced in single or polycrystalline form via aqueous chemical reaction between the appropriate  $\text{CuX}_2$  salts and stoichiometric amounts of the ligands; further details are given in Refs.<sup>18,23,24</sup>, where structural data derived from X-ray crystallography are also found. Some compounds had crystals large enough to permit measurements with a single, orientated sample (Table I). In other cases, the materials were either polycrystalline or the crystals too small for accurate orientation; therefore samples composed of many randomly-orientated microcrystals, effectively powders, were used. In addition to the characterization described in Refs.<sup>18,23</sup>, sample  $g$ -factors were measured<sup>25</sup> using standard electron paramagnetic resonance (EPR)<sup>26</sup>.

The pulsed-field  $M$  experiments used a 1.5 mm bore, 1.5 mm long, 1500-turn compensated-coil susceptometer, constructed from 50-gauge high-purity copper wire<sup>27,28</sup>.

Compound	$B_c$ (T)	$g$	$J$ (K)	$T_N$ (K)	$ J_\perp/J $
[Cu(HF <sub>2</sub> )(pyz) <sub>2</sub> ]BF <sub>4</sub>	18.0	2.13 ± 0.01	-6.3	1.54	9 × 10 <sup>-4</sup>
[Cu(HF <sub>2</sub> )(pyz) <sub>2</sub> ]ClO <sub>4</sub> $B_\perp$	19.1	2.30 ± 0.01	-7.3	1.94	2 × 10 <sup>-3</sup>
[Cu(HF <sub>2</sub> )(pyz) <sub>2</sub> ]ClO <sub>4</sub> $B_\parallel$	20.9	2.07 ± 0.01	-7.2	1.94	2 × 10 <sup>-3</sup>
[Cu(HF <sub>2</sub> )(pyz) <sub>2</sub> ]PF <sub>6</sub>	35.5	2.11 ± 0.01	-12.4	4.31	1 × 10 <sup>-2</sup>
[Cu(HF <sub>2</sub> )(pyz) <sub>2</sub> ]SbF <sub>6</sub>	37.6	2.11 ± 0.01	-13.3	4.31	9 × 10 <sup>-3</sup>
[Cu(HF <sub>2</sub> )(pyz) <sub>2</sub> ]AsF <sub>6</sub>	36.1	2.16 ± 0.02	-12.9	4.34	1 × 10 <sup>-2</sup>
[Cu(py <sub>o</sub> ) <sub>2</sub> (pyz) <sub>2</sub> ](ClO <sub>4</sub> ) <sub>2</sub> $B_\perp$	20.8	2.30 ± 0.01	-7.9	< 2.0	≲ 10 <sup>-3</sup>
[Cu(py <sub>o</sub> ) <sub>2</sub> (pyz) <sub>2</sub> ](ClO <sub>4</sub> ) <sub>2</sub> $B_\parallel$	22.2	2.07 ± 0.01	-7.6	< 2.0	≲ 10 <sup>-3</sup>
CuF <sub>2</sub> (pyz)(H <sub>2</sub> O) <sub>2</sub> $B_\perp$	33.1	2.09 ± 0.02	-11.6	2.54	3 × 10 <sup>-4</sup>
CuF <sub>2</sub> (pyz)(H <sub>2</sub> O) <sub>2</sub> $B_\parallel$	28.8	2.42 ± 0.01	-11.5	2.54	4 × 10 <sup>-4</sup>
Cu(py <sub>z</sub> ) <sub>2</sub> (ReO <sub>4</sub> ) <sub>2</sub>	42.7	2.10 ± 0.05	-14.9	4.2	3 × 10 <sup>-3</sup>
Cu(py <sub>z</sub> ) <sub>2</sub> (H <sub>2</sub> O) <sub>2</sub> Cr <sub>2</sub> O <sub>7</sub>	13.3	2.13 ± 0.01	-4.7	< 1.6	≲ 1 × 10 <sup>-2</sup>

TABLE I: The quasi-2D magnets studied in this work, along with their saturation fields  $B_c$  and  $g$ -factors (here pyz is pyrazine, pyo is pyridine-N-oxide). Data for oriented single crystals are indicated by  $B_\parallel$  ( $B$  parallel to 2D layers) and  $B_\perp$  ( $B$  perpendicular to 2D layers); other data are for powders. In the latter cases, an average  $g$  was evaluated from single-crystal EPR data using standard formulae<sup>26</sup>. The intralayer exchange energy is calculated using Eq. 2; typical uncertainties in the values of  $J$  resulting from uncertainties in  $g$  and  $B_c$  are  $\pm 0.1$  K. Neél temperatures  $T_N$  were measured to  $\pm 0.04$  K using  $\mu$ SR<sup>22</sup>, apart from Cu(py<sub>z</sub>)<sub>2</sub>(ReO<sub>4</sub>)<sub>2</sub>, where the transition was observed in heat capacity data<sup>23</sup> (typical uncertainty  $\pm 0.1$  K). The anisotropy  $|J_\perp/J|$  calculated using Eq. 3.

When a sample is within the coil, the signal is  $V \propto (dM/dt)$ , where  $t$  is the time. Numerical integration is used to evaluate  $M$ .<sup>27</sup> The sample is mounted within a 1.3 mm diameter ampoule that can be moved in and out of the coil<sup>27</sup>. Accurate values of  $M$  are obtained by subtracting empty coil data from that measured under identical conditions with the sample present.

Fields were provided by the 65 T short-pulse and 100 T multi-shot magnets at NHMFL Los Alamos<sup>29</sup> and a 60 T short-pulse magnet at Oxford. The susceptometer was placed within a <sup>3</sup>He cryostat providing  $T$ s down to 0.4 K.  $B$  was measured by integrating the voltage induced in a ten-turn coil calibrated by observing the de Haas-van Alphen oscillations of the belly orbits of the copper coils of the susceptometer<sup>28</sup>.

In the cases that sufficient quantities of material were available, Neél temperatures  $T_N$  were measured using the zero-field muon-spin rotation ( $\mu$ SR) techniques described in Ref.<sup>22</sup> (see also Refs.<sup>19,24</sup>); the results are given in Table I. Ref.<sup>22</sup> also discusses the difficulties encountered when using more conventional techniques to find  $T_N$  in quasi-2D magnets.

### III. EXPERIMENTAL RESULTS

Typical  $M(H)$  data are shown in Fig. 1; all compounds studied (Table I) behaved in a very similar fashion. At higher  $T$ ,  $M(B)$  is convex, showing a gradual approach to saturation at high  $B$ . However, as  $T \rightarrow 0$ , the  $M(B)$  data become concave at lower  $B$ , with a sharp, “elbow”-like transition to a constant saturation magnetization  $M_{\text{sat}}$  at higher  $B$ ; no further changes in  $M$  occur to fields of 85 T with the current materials. We label the field at

which the “elbow” occurs  $B_c$ . As shown in Fig. 1b,  $B_c$  depends on the crystal’s orientation in the field. However, in such cases, the  $M$  data become identical to within experimental accuracy when plotted as  $M/M_{\text{sat}}$  versus  $gB$ , where  $g$  is the  $g$ -factor appropriate for that direction of  $B$  (Fig. 1(c) and Table I). This suggests that the  $g$ -factor anisotropy is responsible for the observed angle dependence of  $B_c$ .

### IV. MONTE-CARLO SIMULATIONS OF MAGNETIZATION DATA

The magnetic properties of the materials in Table I are well described by  $S = \frac{1}{2}$  Cu<sup>2+</sup> spins on a square lattice. The layers are arranged in a tetragonal structure<sup>18</sup>; coupling between the layers depends on the packing of the molecules between. To model data such as those in Fig. 1, we assume that the interaction between the spins is purely Heisenberg-like<sup>1</sup>, resulting in the Hamiltonian

$$\mathcal{H} = J \sum_{\langle i,j \rangle_{xy}} \mathbf{S}_i \cdot \mathbf{S}_j + J_\perp \sum_{\langle i,j \rangle_z} \mathbf{S}_i \cdot \mathbf{S}_j - h \sum_i S_i^z \quad (1)$$

where  $J$  ( $J_\perp$ ) is the strength of the intra- (inter-) planar coupling and  $h = g\mu_B B$  is the Zeeman energy provided by the (uniform) magnetic induction  $B$ . The first (second) summation refers to summing over all nearest neighbors parallel (perpendicular) to the 2D  $xy$ -plane. The dependence of  $M$  as a function of  $B$  is studied for a range of values of  $J_\perp/J$  [from  $J_\perp = 0$  (completely decoupled layers) to  $J_\perp/J = 1$ ] using large-scale numerical simulations. Note that the orientation of  $B$  only affects  $h$  through the anisotropy of the  $g$ -factor, in agreement with the discussion of Fig 1(c) above.

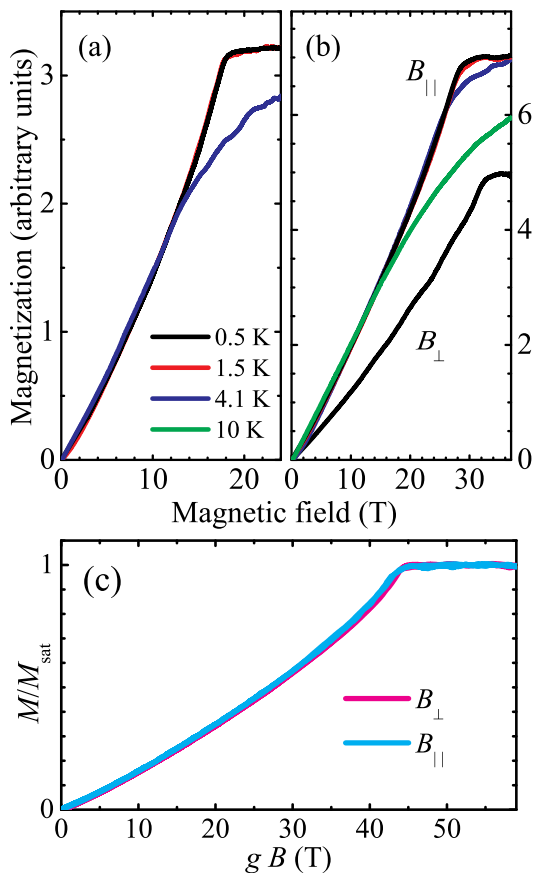


FIG. 1: (a) Magnetization  $M$  of  $[\text{Cu}(\text{HF}_2)(\text{pyz})_2](\text{BF}_4)$  powder versus field  $B$ ; data for  $T = 0.5, 1.5$  and  $4.1$  K are shown (traces for  $0.5$  and  $1.5$  K overlap). (b) Magnetization of  $[\text{CuF}_2(\text{pyz})](\text{H}_2\text{O})_2$  single crystals with  $B$  applied parallel (upper 4 traces) and perpendicular (lower trace,  $0.5$  K) to the 2D planes. Data for  $T = 0.5, 1.5, 4.1$  and  $10$  K are shown for the  $B_{\parallel}$  case. The “elbow” denoting saturation occurs at  $B_c = 28.8$  T for  $B_{\parallel}$  and  $B_c = 33.1$  T for  $B_{\perp}$ . (c) Normalized  $M$  data ( $T = 0.5$  K) for  $[\text{Cu}(\text{HF}_2)(\text{pyz})_2]\text{ClO}_4$  single crystals versus  $gB$ , where  $g$  is the appropriate  $g$ -factor, for  $B$  parallel ( $B_{\parallel}$ ) and perpendicular ( $B_{\perp}$ ) to the layers.

The stochastic series expansion (SSE) method<sup>30,31</sup> is a finite- $T$  Quantum Monte Carlo (QMC) technique based on importance sampling of the diagonal matrix elements of the density matrix  $e^{-\beta H}$ . Using the “operator-loop” cluster update<sup>31</sup>, the autocorrelation time for system sizes considered here (up to  $\approx 3 \times 10^4$  spins) is at most a few Monte Carlo sweeps even at the critical  $T$  for the onset of magnetic order<sup>32</sup>. Estimates of ground state observables are obtained by using sufficiently large values of the inverse  $T$ ,  $\beta$ . We have further found that the statistics of the data obtained can be significantly improved by the use of a tempering scheme<sup>33,34</sup>. We use parallel tempering<sup>34</sup>, where simulations are run simultaneously on a parallel computer, using a fixed value of  $J_{\perp}$  and different, but closely spaced, values of  $h$  over the entire range of fields up to saturation. Along with the usual Monte Carlo

updates, we attempt to swap the values of fields for SSE configurations (processes) with adjacent values of  $h$  at regular intervals (typically after every Monte Carlo step, each time attempting several hundred swaps) according to a scheme that maintains detailed balance in the space of the parallel simulations. This has favorable effects on the simulation dynamics, and reduces the overall statistical errors (at the cost of introducing correlations between the errors, of minor significance here). Implementation of tempering schemes in the context of the SSE method is discussed in Ref.<sup>35</sup>.

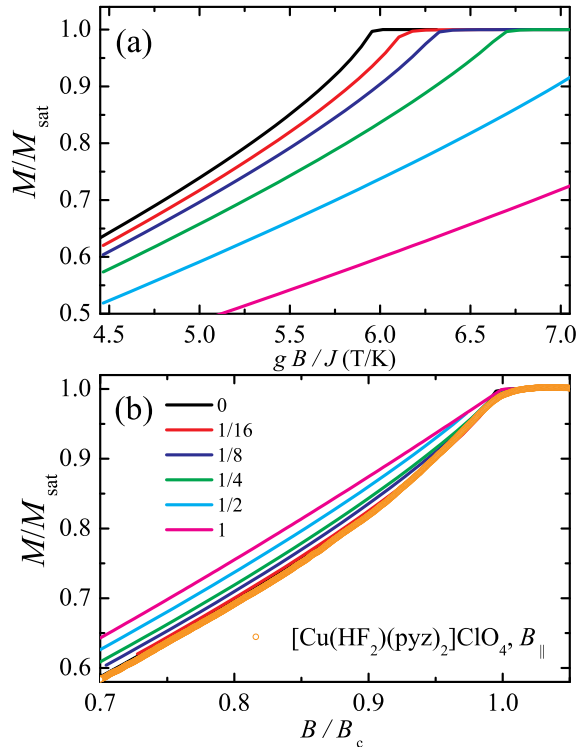


FIG. 2: (a) Calculated magnetization  $M$  of a spin- $\frac{1}{2}$  square lattice with added interlayer anisotropy (see Eq. 1). Simulations are shown for  $J_{\perp}/J = 0$  (uppermost curve)  $\frac{1}{16}, \frac{1}{8}, \frac{1}{4}, \frac{1}{2}$  and  $1$  (lowest curve). Increasing  $J_{\perp}/J$  raises the critical field for saturation  $B_c$  and reduces the curvature of  $M(B)$  below  $B_c$ . (b) Comparison of the model shown in (a) (curves) with experimental data (points) for a  $[\text{Cu}(\text{HF}_2)(\text{pyz})_2]\text{ClO}_4$  crystal ( $T = 0.5$  K, field applied parallel to the 2D planes). Both model and data are plotted in reduced units  $M/M_{\text{sat}}, B/B_c$ . Note that the experimental data lie between the  $J_{\perp}/J = 0$  and  $J_{\perp}/J = \frac{1}{16}$  model curves.

## V. COMPARISONS OF MODEL AND DATA

Fig. 2(a) shows the predictions of the model for low  $T$ , and Fig. 2(b) shows a comparison with typical experimental data. This is made by plotting both model results and experimental data in dimensionless units,  $M/M_{\text{sat}}$  and  $B/B_c$ . As  $M_{\text{sat}}$  is known, there is in effect only one

fit parameter,  $B_c$ . The value of  $B_c$  is varied until there is a satisfactory overlap of the data and one of the model curves<sup>36</sup>. The curvature of the data and the presence of the “elbow” place tight constraints on such a comparison; that in Fig 2(b) is typical of all of the materials in Table I, with their  $M(B)$  data falling between, or closest to, the  $J_\perp/J = 0$  or  $J_\perp/J = \frac{1}{16}$  numerical curves, indicating a high degree of anisotropy. We shall give further justification for this assertion below.

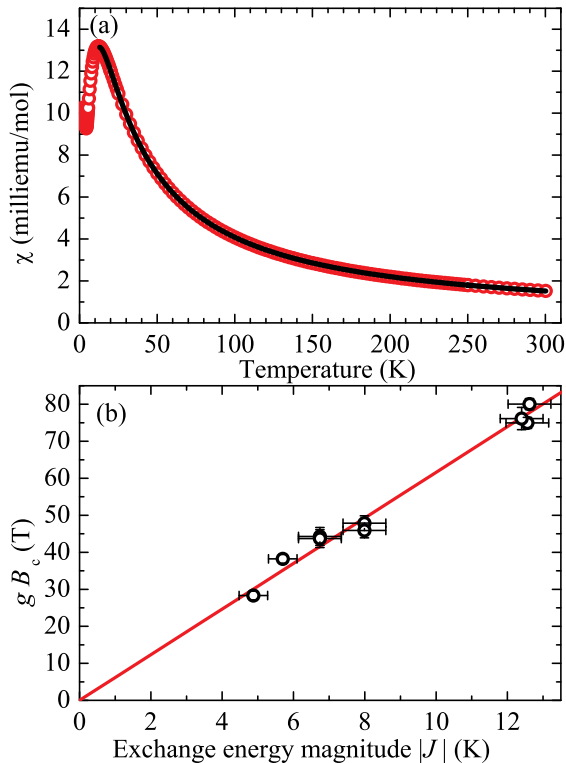


FIG. 3: (a) Temperature dependence of the low-field susceptibility  $\chi$  of  $[\text{Cu}(\text{HF}_2)_2(\text{pyz})_2]\text{SbF}_6$  (points) fitted to the 2D Heisenberg expression (curve) of Ref.<sup>37</sup> to obtain an estimate of  $J$ . (b) Experimental saturation fields times  $g$ -factor ( $gB_c$ ) plotted against values of  $J$  deduced using fits such as that in (a) (points). The straight-line fit to the data yields  $gB_c/|J| = 6.2 \pm 0.2 \text{ TK}^{-1}$ .

For such highly anisotropic magnets, the model predicts the ratio  $gB_c/|J|$  to take values in the range  $5.95 \text{ TK}^{-1}$  ( $J_\perp = 0$ ) to  $6.10 \text{ TK}^{-1}$  ( $J_\perp/J = \frac{1}{16}$ ). Since the experimental uncertainties involved in the location of  $B_c$  are  $\sim 1 - 2\%$ , and the errors in  $g$  are  $\sim 1\%$ , no significant loss in accuracy occurs if we employ the mean value,

$$\frac{gB_c}{|J|} \approx 6.03 \text{ TK}^{-1}, \quad (2)$$

in what follows. To check the model prediction, a fit of the  $T$ -dependent low-field susceptibility following the method of Ref.<sup>37</sup> was used to determine  $J$  independently for a selection of compounds (Fig. 3(a))<sup>38</sup>; the values

obtained are compared with  $gB_c$  in Fig 3(b). As can be seen, the points lie close to the line  $gB_c/|J| = 6.2 \pm 0.2 \text{ TK}^{-1}$ , in good agreement with the predicted value (Eq. 2). As noted above, it is possible to determine the value of  $B_c$  to a very good accuracy ( $\pm 1 - 2\%$ ); once the dimensionality of the magnet in question is seen to fall within the limits  $J_\perp/J \approx 0 - \frac{1}{16}$  using fits such as those in Fig. 2(b), Eq. 2 almost certainly presents the most accurate method for evaluating  $J$ . Intralayer exchange energies  $J$  derived in this way from measured values of  $g$  and  $B_c$  are in Table I.

Finally, an estimate of the anisotropy  $|J_\perp/J|$  can be made using the results of quantum-Monte-Carlo simulations of quasi-2D Heisenberg antiferromagnets<sup>39</sup>, which found

$$\frac{|J_\perp|}{|J|} = \exp\left(2.43 - 2.30 \times \frac{|J|}{T_N}\right), \quad (3)$$

where both  $|J|$  and  $T_N$  are measured in K; the resulting values are given in Table I. Note that Eq. 3 is a rapidly-varying function of  $|J|/T_N$ ; small shifts in either parameter result in quite large changes in  $|J_\perp/J|$ . Given the experimental and other errors in  $J$  and  $T_N$  ( $\sim$  a few %), the derived values of  $|J_\perp/J|$  will probably be within a factor  $\sim 2$  of the true values. In spite of this  *caveat* , the  $|J_\perp/J|$  values in Table I are all  $\lesssim 0.01$ , in good agreement with the fits to the magnetization data (e.g. Fig 2) that suggested  $0 \lesssim |J_\perp/J| \lesssim \frac{1}{16}$  for all of the compounds.

## VI. SYSTEMATIC TRENDS IN THE $[\text{Cu}(\text{HF}_2)(\text{PYZ})_2]\text{X}$ FAMILY

Having established a reliable method for deriving  $J$  and the anisotropy from  $M(B)$  and  $T_N$ , we focus our remaining discussion on the compounds with formula  $[\text{Cu}(\text{HF}_2)(\text{pyz})_2]\text{X}$ ,<sup>18,23</sup> where X can be  $\text{ClO}_4$ ,  $\text{BF}_4$ ,  $\text{PF}_6$  *etc.* (Table I). All of these materials possess very similar extended polymeric structures consisting of 2D, four-fold symmetric  $[\text{Cu}(\text{pyz})_2]^{2+}$  sheets in the  $ab$ -planes that are connected along the  $c$ -axis by linearly-bridging  $[\text{HF}_2]^-$  ions (Fig. 4)<sup>18,23</sup>. The Cu-Cu separations are similar along the Cu-(pyz)-Cu (0.6852 nm) and Cu-FHF-Cu (0.6619 nm) linkages, so that the structure may be described as pseudo-cubic<sup>18,23</sup>; the X anions are placed in the body-centre positions within each “cube”. The Cu-F and Cu-(pyz) bonds result in the  $\text{Cu}^{2+} d_{x^2-y^2}$  orbitals lying within the  $ab$  planes, as evidenced by the  $g$ -factor anisotropy observed in EPR measurements<sup>25</sup>; as noted above, the  $ab$  planes also correspond to the 2D planes within which the strong exchange pathways occur.

There is little variation of the lattice parameters across the  $[\text{Cu}(\text{HF}_2)(\text{pyz})_2]\text{X}$  series<sup>18,23</sup>; given this similarity, it is at first sight surprising that the exchange parameters  $J$  in Table I fall into two distinct groups: the compounds with tetrahedral anions (X =  $\text{BF}_4$  and  $\text{ClO}_4$ ) possess values  $J \approx -7$  K and those with octahedral anions (X =  $\text{PF}_6$ ,  $\text{SbF}_6$  and  $\text{AsF}_6$ ) have  $J \approx -13$  K. Note also

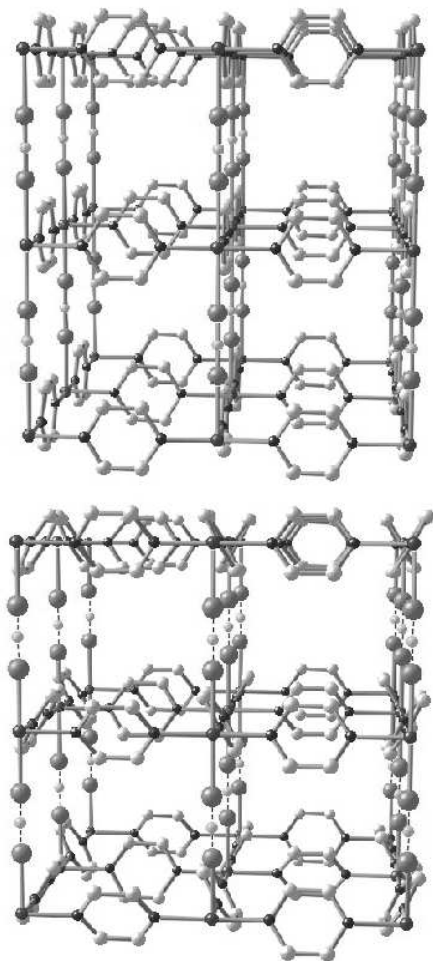


FIG. 4: Experimentally-determined<sup>18,23</sup> room-temperature crystal structures of  $[\text{Cu}(\text{HF}_2)(\text{pyz})_2]\text{X}$  2D organic magnets. In each figure, the Cu-F-H-F-Cu linkages (parallel to  $c$  and perpendicular to the  $ac$  planes) are vertical. The upper figure is for  $\text{X} = \text{SbF}_6$  whilst the lower shows  $\text{X} = \text{BF}_4$ . Note that for  $\text{X} = \text{BF}_4$  (lower), the planes of the pyrazine molecules are tilted by  $31.6^\circ$  away from being orthogonal to the  $ab$  planes. However, for  $\text{X} = \text{SbF}_6$  (upper), the planes of the pyrazine molecules are perpendicular to the  $ab$  planes. (The  $[\text{SbF}_6]^-$  and  $[\text{BF}_4]^-$  anions have been omitted for clarity; they inhabit the “body-center” sites of each approximately cubic unit.)

that the compounds with tetrahedral anions are more anisotropic ( $|J_\perp/J| \sim 10^{-3}$ ) than those with octahedral anions ( $|J_\perp/J| \sim 10^{-2}$ ).

We first discuss whether the X anions can play a direct role as exchange pathways between the  $\text{Cu}^{2+}$  ions. First of all, the anions  $[\text{ClO}_4]^-$  and  $[\text{BF}_4]^-$  have radically different electronic orbitals, and yet the intralayer exchange energies for the magnets containing these anions are very similar (see the first three rows of Table I). Moreover, as mentioned above, the X anions are not within the 2D  $\text{Cu}^{2+}$  planes, but at body-center positions within the “cubes” (Fig. 4). The Cu-(anion) separation is therefore roughly the same for the interlayer and intralayer direc-

tions; if the anions played a direct role as exchange pathways, one might expect that the  $[\text{Cu}(\text{HF}_2)(\text{pyz})_2]\text{X}$  compounds would have  $|J_\perp/J|$  values that were somewhat larger (i.e. more isotropic) than the values  $\sim 10^{-3} - 10^{-2}$  that are actually observed (see Table I). Therefore, instead of playing a direct role in the exchange, it is more likely that it is an anion *size effect* on the crystal structure that is affecting the exchange pathways.

The structural difference that may well be responsible for the factor of two change in  $J$  is the configuration of the pyrazine molecules within the Cu-(pyz)-Cu linkages. Fig. 4 (upper) shows  $[\text{Cu}(\text{HF}_2)(\text{pyz})_2]\text{SbF}_6$ , one of the systems with octahedral anions; the structures of  $\text{X} = \text{AsF}_6$ ,  $\text{PF}_6$  are very similar. At room temperature, the larger size of the octahedral anions compared to the tetrahedral examples forces the pyrazine ligands to stand up virtually perpendicular to the  $ab$  planes<sup>23</sup> (Fig. 4). By contrast, the planes of the pyrazine ligands in the compounds with the smaller tetrahedral anions,  $[\text{Cu}(\text{HF}_2)(\text{pyz})_2]\text{BF}_4$  (Fig. 4 (lower)) and  $[\text{Cu}(\text{HF}_2)(\text{pyz})_2]\text{ClO}_4$ , are not perpendicular to the  $ab$  plane, but are tilted away by  $31.6^\circ$  ( $\text{X} = \text{BF}_4$ ) or  $25.8^\circ$  ( $\text{X} = \text{ClO}_4$ ) in a pattern that preserves the four-fold symmetry of the  $\text{Cu}^{2+}$  sites<sup>23</sup>. As one lowers the temperature<sup>23</sup>, the tilt of the pyrazine ligands increases in all of the compounds (i.e. those with octahedral and tetrahedral anions); however, in the case of the octahedral anions, space-filling considerations restrict the tilt to values in the range  $5^\circ$  ( $\text{X} = \text{PF}_6$ ) to  $12^\circ$  ( $\text{X} = \text{AsF}_6$ ). This suggests that it may be the orientation dependence of the pyrazine ligand that produces the factor two difference in  $J$ , with the more perpendicularly-disposed pyrazines (Fig. 4) presenting a more efficient exchange pathway within the layers.

## VII. SUMMARY

Magnetization experiments have been carried out on nine organic Cu-based 2D Heisenberg magnets. These systems exhibit a low- $T$  magnetization that is concave as a function of field, with a sharp “elbow” transition to a constant saturation value at a critical field  $B_c$ . Monte-Carlo simulations including interlayer exchange quantitatively reproduce the data; the concavity indicates the effective dimensionality and  $B_c$  is an accurate measure of the in-plane exchange energy  $J$ . Taken in conjunction with Néel temperatures derived from muon-spin rotation, the values of  $J$  may be used to obtain quantitative estimates of the exchange anisotropy,  $|J_\perp/J|$ .

We suggest that in organic magnets of the form  $[\text{Cu}(\text{HF}_2)(\text{pyz})_2]\text{X}$ , where X is an anion molecule, the sizes of  $J$  and  $J_\perp$  may be controlled by the tilting of the pyrazine molecule with respect to the 2D planes. Thus, it may be possible to use molecular architecture to design magnets with very specific values of  $J$ , tailored to a particular desired property. One possible application would be an organic magnet designed to simulate the antifer-

romagnetic interactions germane to cuprate superconductivity<sup>3,10,11,12,13,14</sup>, but with exchange energies small enough to permit manipulation of the magnetic ground-state using standard laboratory fields.

### Acknowledgements

We thank Peter Baker and Alex Amato for experimental assistance and Bill Hayes for stimulating discussions. This work is supported by the US Department of Energy (DoE) BES program ‘‘Science in 100 T’’. Work at

NHMFL occurs under the auspices of the National Science Foundation, DoE and the State of Florida. Work at Argonne is supported by the Office of Basic Energy Sciences, DoE (contract DE-AC02-06CH11357). Part of this work was carried out at the Swiss Muon Source, Paul Scherrer Institut, CH, and at the ISIS Facility, Rutherford-Appleton Laboratory, UK. Research at EWU was supported by an award from the Research Corporation. TL and PAG acknowledge support from the Royal Commission of the Exhibition of 1851 and the Glasstone Foundation respectively. JS thanks Oxford University for the provision of a Visiting Professorship.

- 
- <sup>1</sup> M.A. Kastner, R.J. Birgenau, G. Shirane and Y. Endoh, *Rev. Mod. Phys.* **70**, 897 (1998).
- <sup>2</sup> U. Schollwöck, D.J.J. Farnell and R.F. Bishop (eds), *Quantum magnetism*, (Springer, Berlin, 2004).
- <sup>3</sup> E. Manousakis, *Rev. Mod. Phys.* **53**, 1 (1991).
- <sup>4</sup> N.B. Christensen, H.M. Ronnow, D.F. McMorrow, A. Harrison, T.G. Perring, M. Enderle, R. Coldea, L.P. Regnault and G. Aeppli, *Proc. Nat. Acad. Sci.* **104**, 15264 (2007).
- <sup>5</sup> O.P. Vajk, P.K. Mang, M. Greven, P.M. Gehring and J.W. Lynn, *Science* **295**, 1691 (2002).
- <sup>6</sup> D.S. Deng, X.F. Jin and R. Tao, *Phys. Rev. B* **65**, 132406 (2002).
- <sup>7</sup> B.B. Beard, A. Cuccoli, R. Vaia and P. Verrucchi, *Phys. Rev. B* **68**, 104406 (2003).
- <sup>8</sup> P. Sengupta, A.V. Sandvik and R.R.P. Singh, *Phys. Rev. B* **68**, 094423 (2003).
- <sup>9</sup> R. Zhang and S. Zhu, *Phys. Lett. A* **348**, 110 (2006).
- <sup>10</sup> J.R. Schrieffer and J.S. Brooks (eds), *High temperature superconductivity theory and experiment* (Springer, Berlin, 2007).
- <sup>11</sup> P. Dai, H.A. Mook, R.D. Hunt and F. Doğan, *Phys. Rev. B* **63**, 054525 (2001).
- <sup>12</sup> C. Stock, W.J.L. Buyers, R.A. Cowley, P.S. Clegg, R. Coldea, C.D. Frost, R. Liang, D. Peets, D. Bonn, W.N. Hardy and R.J. Birgenau, *Phys. Rev. B* **71**, 024522 (2005).
- <sup>13</sup> S.R. Julian and M. Norman, *Nature* **447**, 537 (2007).
- <sup>14</sup> N.Harrison, R.D. McDonald and J. Singleton, preprint arXiv:0710.1932 (2007).
- <sup>15</sup> P.Monthoux, D. Pines and G.G. Lonzarich, *Nature* **450**, 1177 (2007).
- <sup>16</sup> N.D. Mermin and H. Wagner, *Phys. Rev. Lett.* **17**, 1133 (1966).
- <sup>17</sup> J. Choi, J.D. Woodward, J.L. Musfeldt, C.P. Landee and M.M. Turnbull, *Chem. of Materials* **15**, 2797 (2003).
- <sup>18</sup> J.L. Manson, M.M. Conner, J.A. Schlueter, T. Lancaster, S.J. Blundell, M.L. Brooks, T. Papageorgiou, A.D. Bianchi, J. Wosnitzer and M.H. Wangbo, *Chem. Comm.* **2006**, 4894 (2006).
- <sup>19</sup> T. Lancaster, S.J. Blundell, M.L. Brooks, P.J. Baker, F.L. Pratt, J.L. Manson, M.M. Conner, F. Xiao, C.P. Landee, F.A. Chaves, S. Soriano, M.A. Novak, T.P. Papageorgiou, A.D. Bianchi, T. Herrmannsdörfer, J. Wosnitzer and J.A. Schlueter, *Phys. Rev. B* **75**, 094421 (2007).
- <sup>20</sup> M. Deumel, C.P. Landee, J.J. Novoa, M.A. Robb and M.M. Turnbull, *Polyhedron* **22**, 2235 (2003).
- <sup>21</sup> T. Lancaster, S.J. Blundell, M.L. Brooks, P.J. Baker, F.L. Pratt, J.L. Manson, C.P. Landee and C. Baines, *Phys. Rev. B* **73**, 020410 (2006).
- <sup>22</sup> S.J. Blundell, T. Lancaster, F.L. Pratt P.J. Baker, M.L. Brooks, C. Baines, J.L. Manson and C.P. Landee, *J. Phys. Chem. Solids*, **68**, 2039 (2007).
- <sup>23</sup> J.L. Manson, H. Southerland, J. Schlueter and K. Funk, preprint (2008).
- <sup>24</sup> T. Lancaster, S.J. Blundell, P.J. Baker, M.L. Brooks, W. Hayes, F.L. Pratt, J.L. Manson M.M. Conner and J.A. Schlueter, *Phys. Rev. Lett.* **99**, 267601 (2007).
- <sup>25</sup> S. Cox, R.D. McDonald, K. Funk, H.A. Southerland, J.L. Manson and J.A. Schlueter, preprint (2008).
- <sup>26</sup> A. Abragam et B. Bleaney, *Résonance paramagnétique électronique des ions de transition* (Presses Universitaires de France, Paris, 1971), p 208.
- <sup>27</sup> P.A. Goddard, J. Singleton, A.L. Lima-Sharma, E. Morosan, S.J. Blundell, S.L. Bud’ko and P.C. Canfield, *Phys. Rev. B.*, **75**, 094426 (2007).
- <sup>28</sup> P.-C. Ho, J. Singleton, M.B. Maple, H. Harima, P.A. Goddard, Z. Henkie and A. Pietraszko, *New J. Physics*, **9**, 269 (2007).
- <sup>29</sup> M. Jaime, A. Lacerda, Y. Takano and G.S. Boebinger, *Institute of Physics: Conference Series* **51**, 643 (2006).
- <sup>30</sup> A. W. Sandvik and J. Kurkijärvi, *Phys. Rev. B* **43**, 5950 (1991); A. W. Sandvik, *ibid.* **56**, 11678 (1997).
- <sup>31</sup> A. W. Sandvik, *Phys. Rev. B* **59**, R14157 (1999).
- <sup>32</sup> O. F. Syljuåsen and A. W. Sandvik, *Phys. Rev. E* **66**, 046701 (2002).
- <sup>33</sup> E. Marinari, *Lecture Notes in Physics*, Vol. 501 *Advances in computer simulation: lectures held at the Eötvös Summer School in Budapest, Hungary, 16-20, July 1996*, edited by J. Kertsz and I. Kondor (Springer, 1998).
- <sup>34</sup> K. Hukushima, H. Takayama, K. Nemoto, *Int. J. Mod. Phys. C* **7**, 337 (1996); K. Hukushima, K. Nemoto, *J. Phys. Soc. Jpn.* **65**, 1604 (1996)
- <sup>35</sup> P. Sengupta, A. W. Sandvik, and D. K. Campbell, *Phys. Rev. B* **65**, 155113 (2002).
- <sup>36</sup> From Eq. 1 it is easy to see that  $g\mu_B B_c = 4J + 2J_\perp$ . However, without the information on the anisotropy given by the curvature of the  $M(B)$  data, this expression contains two unknowns. Moreover, it was found that the best method (i.e. that with the smallest uncertainties and that best utilized all of the data) for determining  $B_c$  was that described in the text; matching the  $M(B)$  curves to the Monte Carlo simulations by varying  $B_c$ .

- <sup>37</sup> C.P. Landee, S.A. Roberts and R.D. Willett, J. Chem. Phys. **68**, 4574 (1978).
- <sup>38</sup> The definition of  $J$  used in Ref.<sup>37</sup> differs by a factor 2 from the one employed in the present paper.
- <sup>39</sup> C. Yasuda, S. Todo, K. Hukushima, A. Alet, M. Keller M. Troyer and H. Takayama, Phys. Rev. Lett. **94**, 217201 (2005).